HHS Public Access

Author manuscript

Cell Rep. Author manuscript; available in PMC 2019 April 03.

Published in final edited form as:

Cell Rep. 2019 March 26; 26(13): 3629–3642.e4. doi:10.1016/j.celrep.2019.02.108.

Single-Cell Resolution and Quantitation of Targeted Glucocorticoid Delivery in the Thymus

Matthew D. Taves[1], **Paul R. Mittelstadt**[1], **Diego M. Presman**[2,3], **Gordon L. Hager**[2], and **Jonathan D. Ashwell**[1,4,*]

[1]Laboratory of Immune Cell Biology, Center for Cancer Research, National Cancer Institute, NIH, Bethesda, MD 20892, USA

[2]Laboratory of Receptor Biology and Gene Expression, Center for Cancer Research, National Cancer Institute, NIH, Bethesda, MD 20892, USA

[3]Instituto de Fisiología, Biología Molecular y Neurosciencias (IFIBYNE-UBA-CONICET), Universidad de Buenos Aires, Facultad de Ciencias Exactas y Naturales, Buenos Aires, Argentina

[4]Lead Contact

SUMMARY

Glucocorticoids are lipid-soluble hormones that signal via the glucocorticoid receptor (GR), a ligand-dependent transcription factor. Circulating glucocorticoids derive from the adrenals, but it is now apparent that paracrine glucocorticoid signaling occurs in multiple tissues. Effective local glucocorticoid concentrations and whether glucocorticoid delivery can be targeted to specific cell subsets are unknown. We use fluorescence detection of chromatin-associated GRs as biosensors of ligand binding and observe signals corresponding to steroid concentrations over physiological ranges *in vitro* and *in vivo*. In the thymus, where thymic epithelial cell (TEC)-synthesized glucocorticoids antagonize negative selection, we find that $CD4^+CD8^+TCR^{hi}$ cells, a small subset responding to self-antigens and undergoing selection, are specific targets of TEC-derived glucocorticoids and are exposed to 3-fold higher levels than other cells. These results demonstrate and quantitate targeted delivery of paracrine glucocorticoids. This approach may be used to assess *in situ* nuclear receptor signaling in a variety of physiological and pathological contexts.

In Brief

Glucocorticoids signal via the GR, a ligand-dependent transcription factor, and paracrine glucocorticoid signaling occurs in the thymus. Taves et al. use chromatin-associated GRs as biosensors to estimate glucocorticoid concentrations in vitro and in vivo. In the thymus, antigen-

*Correspondence: jda@pop.nci.nih.gov.

AUTHOR CONTRIBUTIONS

M.D.T., P.R.M., and J.D.A. conceived and designed experiments. M.D.T. performed the experiments. P.R.M., D.M.P., and G.L.H. contributed reagents. M.D.T. and J.D.A. analyzed the data and wrote the paper.

SUPPLEMENTAL INFORMATION

Supplemental Information can be found online at https://doi.org/10.1016/j.celrep.2019.02.108.

DECLARATION OF INTERESTS

The authors declare no competing interests.

signaled $CD4^{+}8^{+}TCR^{hi}$ cells are targeted by epithelial cell-synthesized glucocorticoids to promote positive selection.

Graphical Abstract

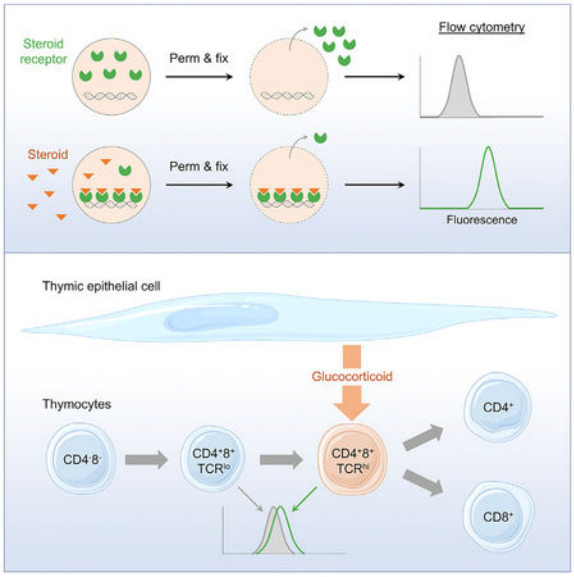

INTRODUCTION

Glucocorticoids are adrenal-derived steroid hormones that are required for organismal development and homeostasis. Glucocorticoids function primarily as the activating ligand of the glucocorticoid receptor (GR), a ubiquitously expressed ligand-dependent transcription factor. Glucocorticoid binding to the cytosolic GR induces a change in GR conformation, release from chaperone proteins, exposure of a nuclear localization sequence, and trafficking to the nucleus. In the nucleus, liganded GR forms homodimers and homotetramers, and binds to specific DNA sequences in gene promoters to initiate or repress gene expression, either directly as a bona fide transcription factor or by interacting with and regulating other transcription factors (Presman et al., 2014). Whereas high physiological ligand concentrations drive nearly all GRs to the nucleus (Stavreva et al., 2009), only 20%–45% of the nuclear-localized GR is estimated to be bound to chromatin at any given time (Paakinaho et al., 2017).

Most research regarding glucocorticoids *in vivo* has dealt with the circulating hormone, which is derived from the adrenals. There is, however, a growing appreciation that glucocorticoids are synthesized by a large number of extra-adrenal tissues, and that this tissue-specific production is critical for local control of immune activation (Noti et al., 2009; Taves et al., 2011a). An example of the importance of tissue-specific GR signaling is the thymus, in which the GR is required for generation of competent T cells, which orchestrate adaptive immunity. Glucocorticoids dampen the consequences of signaling by T cell antigen receptors (TCRs) with high affinity for self-antigens, allowing cells that would otherwise undergo apoptotic death (negative selection) to survive and become mature T cells (positive

selection) (Mittelstadt et al., 2012, 2018). Within the thymus, glucocorticoids are produced by thymic epithelial cells (TECs) (Vacchio et al., 1994; Lechner et al., 2000), and in early life this local synthesis can result in a higher local glucocorticoid level than in the blood (Schmidt and Soma, 2008; Taves et al., 2015, 2016a). The importance of locally derived glucocorticoids was demonstrated by deletion of the terminal enzyme in *de novo* glucocorticoid biosyn-thesis, Cyp11b1, in TECs. Despite normal circulating glucocorticoid levels, antigen-specific thymocyte development was altered in a manner similar to that in mice whose thymocytes lack the GR and are therefore unable to respond to glucocorticoids (Mittelstadt et al., 2018). TEC-derived glucocorticoids are thus critical for immunocompetence. Dissecting the mechanism of paracrine and autocrine glucocorticoid signaling in the thymus and other tissues, however, has been obstructed by the inability to measure steroid signaling with high resolution. Currently, two main approaches are used to examine tissue steroid signaling: (1) direct measurement of total tissue steroids, and (2) measurement of steroid-dependent responses. Direct measurement of local steroid levels (e.g., in rapidly collected and frozen tissue samples) has excellent temporal resolution, but the highest spatial resolution is currently obtained from dissected (Amateau et al., 2004; Croft et al., 2008; Prior et al., 2013; Tobiansky et al., 2018) or whole (Taves et al., 2015, 2016a) organ samples, from which total steroid content is extracted and selected steroids measured by immunoassays or mass spectrometry. These approaches thus obtain aggregate measures of steroid concentrations averaged over thousands or millions of cells and extracellular material, and may not reflect the bioavailable steroid fraction. Mass spectrometry imaging may offer improved spatial specificity for high-concentration analytes (Cobice et al., 2013), but still provides similar averaged values. In contrast, measurement of steroid responses can have excellent spatial resolution, but at the cost of specificity and temporal resolution. Steroid-dependent gene expression in particular can be measured in single cells, but such responses are cell specific and context dependent (Weikum et al., 2017), and mRNA decay may take many hours (Yang et al., 2003). Across tissues, therefore, it remains unknown which cell subsets are signaled by glucocorticoids, whether paracrine glucocorticoid delivery is targeted, and what concentrations cells within an organ are exposed to.

Detection of numerous signaling molecules has advanced greatly with the development of biosensors, which transform biochemical information into analytically useful signals (Thévenot et al., 2001). Fluorescent biosensors, for example, allow imaging and quantification in living cells with high spatial and temporal resolution, and are used to detect the activity of signaling intermediates such as cAMP, glutamate, tryptophan, and Ca^{2+} (VanEngelenburg and Palmer, 2008). They can also be used to detect the activities of proteins such as GTPases (Mochizuki et al., 2001), kinases (Wang et al., 2005), and caspases (Zhang et al., 2013). We hypothesized that ligand-dependent association with nuclear chromatin might allow us to selectively detect occupied GRs, thus allowing endogenous GRs to function as biosensors for their ligand. Here, we used chromatin-associated GR for single-cell detection and quantification of glucocorticoid signaling, identifying targeted delivery of TEC-derived glucocorticoids to a small subset of thymocytes undergoing antigen-specific selection.

RESULTS

Simultaneous Permeabilization and Fixation Preferentially Retains the Liganded GR

It is difficult to distinguish between biologically active and inactive GRs at the single-cell level. Because ligand binding stimulates GR interaction with DNA, and because protein-DNA interactions are effectively stabilized by formaldehyde cross-links (Hoffman et al., 2015), we hypothesized that a combination of cross-linking and detergent permeabilization would retain liganded, chromatin-bound GR molecules and remove unliganded, freely diffusing GRs. Measurement of GR retention would thus provide a specific biosensor of ligand-dependent activation and could be applied as a cell-specific readout of glucocorticoid exposure. Permeabilization and fixation conditions were tested using 3617 mouse mammary adenocarcinoma cells that stably express a GFP-tagged GR (Presman et al., 2014). Cells were cultured for 15 min in steroid-free medium or medium containing the natural glucocorticoid corticosterone, and GFP-GR levels were assessed by flow cytometry. As expected, corticosterone treatment had no effect on GFP-GR levels in living cells or cells fixed with 2% paraformaldehyde (“Fix only”) (Figure 1A). Sequential permeabilization and then fixation has been used to selectively retain DNA replication proteins (Forment and Jackson, 2015), and although this approach did result in a corticosterone-dependent increase in GFP-GR, >90% of GFP-GR fluorescence was lost and the remaining signal was extremely low (Figure S1A). In contrast, simultaneous permeabilization and fixation with 0.5% Triton X-100 and 2% paraformaldehyde (“Perm-fix”) resulted in a ligand-dependent increase in GFP-GR levels compared with vehicle control and much better GFP-GR retention in the presence or absence of ligand (Figure 1A; Figures S1A and S1B). Sequential permeabilization and fixation may be more suitable for chromatin-cross-linking of replication proteins that have relatively long DNA dwell times (e.g., PCNA) (Ha et al., 2012), whereas simultaneous permeabilization-fixation may be required for chromatin-cross-linking of transcription factors that have shorter DNA dwell times (e.g., GR) (Paakinaho et al., 2017). Varying both the formaldehyde and detergent concentrations revealed that higher formaldehyde concentrations had to be accompanied by stronger permeabilization to give the same ligand-dependent GR retention (Figure 1B). This presumably reflects the need for an optimal balance between the speed of GR fixation and the time it takes for unliganded GR to be washed from the cell, and this balance likely differs between proteins depending on their chromatin-binding characteristics. Methanol-containing formal-dehyde and methanol-free formaldehyde were both suitable (Figure S1C). Interestingly, the commercial BD Cytofix/Cytoperm (“Cytofix”) buffer behaved identically to fix-only, whereas the commercial eBioscience FoxP3 transcription factor buffer set (“TF fixative”) (00–5523) behaved similarly to perm-fix (Figure 1B; Figure S1D).

Permeabilization-Fixation Retains Chromatin-Associated GR

Chemically cross-linked GR could become resistant to washing out by forming large higher-order structures or protein aggregates, or by tethering to adjacent chromatin (Hoffman et al., 2015). To first test whether perm-fix specifically retains nuclear and not cytosolic GR, we examined GFP-GR-expressing 3617 cells using imaging flow cytometry, which combines flow cytometry with fluorescence microscopy. In the absence of glucocorticoids, the GR was primarily found in the cytosol of live cells, but after corticosterone treatment it was largely

nuclear (Figure 2A, Live). Nuclear GR translocation after corticosterone treatment was especially clear in fixed cells, as shown by GFP colocalization with DAPI-stained nuclei (Figure 2A, Fix only). In contrast, although little GR was retained after perm-fix of untreated cells, there was easily detectable GFP-GR in the nuclei of corticosterone-treated cells (Figure 2A, Perm-fix). Quantification of nuclear GFP-GR by the GFP/DAPI similarity score (see STAR Methods) showed a similar frequency of nuclear translocation in fixed and perm-fixed cells (Figure 2A, right). Because only a minority of nuclear-localized GR is chromatin bound at any given time (Paakinaho et al., 2017), if perm-fix primarily cross-links DNA and/or protein-associated GR, the majority should be lost even after corticosterone treatment. Indeed, as judged by immunoblotting, treatment with corticosterone preserved GR compared with medium alone, but it was much reduced compared with cells that were not perm-fixed (Figure 2B). Loss of actin after perm-fix was similar with or without corticosterone, whereas nuclear histone H3 was retained in both live and perm-fixed cells regardless of corticosterone treatment, showing that the effect of glucocorticoid treatment was specific to its receptor.

A specific role for chromatin binding in perm-fix GR retention was indirectly evaluated by incubating 3617 cell lines expressing no GR (KO), wild-type GR (GR^{wt}), or a dimerization-impaired mutant GR (GR^{mon}) that translocates to the nucleus upon glucocorticoid treatment, but only at very high concentrations does it associate with chromatin (Presman et al., 2014). Glucocorticoid treatment did not alter GFP-GR^{wt} or GFP-GR^{mon} levels in live cells as evaluated by flow cytometry (Figure 2C), but a 1,000-fold higher dose was needed for GR^{mon} retention after perm-fix (Figure 2D). The possible requirement for an interaction with chromatin in GR retention was directly tested using HEK293T cells expressing GFP-GR^{wt} (Presman et al., 2014) or a GR mutant (GFP-GR^{C440G}) in which the C440G substitution in the DNA binding domain reduces the affinity for cognate DNA binding sites (Paakinaho et al., 2017). The dose-response of GR retention was similar at lower concentrations of corticosterone, but GFPGR^{C440G} levels plateaued at approximately 30 nM, whereas GFP-GR^{wt} continued to increase. To eliminate any possible contribution of GFP-GR^{C440G} heterodimerization with 293 cell's endogenous wild-type GR, a double mutant (GFP-$GR^{C440G/mon}$) incapable of dimerizing with itself or the endogenous GR was introduced (Figure 2E). In this case, the entire dose-response curve was shifted toward higher corticosterone levels. We therefore conclude that ligand-induced GR retention after perm-fix largely reflects GR cross-linking to chromatin.

Use of Permeabilization-Fixation to Quantitate GR-Chromatin Dissociation Kinetics

The GR dissociates from chromatin within 15 min of ligand removal (Stavreva et al., 2009) but remains in the nucleus for many hours (Liu and DeFranco, 2000). Thus, the rate at which perm-fix retention of GR decreases after ligand removal should reflect the fraction that is chromatin associated (half-life of minutes) versus simply nuclear (half-life of hours). We used the perm-fix assay to determine the kinetics of GR dissociation from chromatin after ligand withdrawal. GFP-GR 3617 cells were treated with corticosterone for 15 min, washed, and incubated in steroid-free medium at room temperature for different times before perm-fix. After corticosterone removal, GR retention decreased with a $t_{1/2}$ of 17 min (Figure 2F). Even 60 min after removing glucocorticoids, the GR remained in the nucleus as

demonstrated by fix-only followed by imaging flow cytometry (Figure 2G). In contrast, after perm-fix the GR was lost from the cell. Thus, the rapid decrease of GR signal in perm-fixed cells after ligand removal reflects a decrease in chromatin-associated GR, not movement of the GR to the cytosol.

Cross-linking of Liganded Nuclear Receptors Quantifies Ligand Exposure

The applicability of perm-fix as a generalizable means of detecting liganded nuclear receptors was assessed with 3617 cells that stably express a variety of fluorescent protein-receptor fusion products: GFP-androgen receptor (AR), mCherry (mCh)-estrogen receptor α (ER), GFP-GR, or GFP-progesterone receptor β (PR) (Presman et al., 2016). Brief (15–30 min) incubation of the cells with their corresponding steroid ligand had no effect on receptor protein levels in live cells, as detected by flow cytometry (Figure 3A; Figure S1E). Fix-only also resulted in little, if any, loss of receptor fluorescence compared with live cells, confirming that receptor proteins were not depleted with this approach. In contrast, after perm-fix there was substantial receptor loss in all groups, but much less so in the cells incubated with ligand (Figure 3A). Of note, the unliganded ER is constitutively located in the nucleus (Htun et al., 1999); therefore, ligand-specific retention of ER after perm-fix is consistent with preferential stabilization of liganded and chromatin-associated receptors, not total nuclear receptors. For all four receptors, dose-response studies found that retention varied as a function of steroid dose (Figure 3B). The ligand-sensitive portions of the fluorescence curves spanned endogenous steroid concentrations (Overk et al., 2013; Taves et al., 2011b), and affinities (K_d) calculated from these data were within the range of values previously determined using competitive radioligand binding assays (Attardi and Ohno, 1976; Philibert and Raynaud, 1973; Reul and de Kloet, 1985; Wasner et al., 1983; Yeakley et al., 1980). GFP-GR fluorescence curves also corresponded with different ligand affinities (Figure 3C), as previously determined using competitive radioligand binding assays (Munck and Brinck-Johnsen, 1968; Russo-Marie et al., 1979). Thus, this approach could be useful for unbiased assessments of nuclear receptor activity in response to a diverse spectrum of ligands, known and potentially unknown.

Permeabilization-Fixation of Primary Cells Allows Antibody Detection of Ligand-Activated GR

The use of fluorescent fusion proteins allowed us to explore the relationship between GR occupancy and retention, but is not applicable to normal tissues. We therefore asked whether GR retention after perm-fix could be detected by antibody staining. Initial experiments using corticosterone-treated GFP-GR^{wt}, GFP-GR^{mon}, and GR-deficient 3617 cells showed that anti-GR staining after perm-fix treatment closely paralleled GFP-GR fluorescence as evaluated by flow cytometry (Figure S2A). Next, experiments were performed with primary murine thymocytes from wild-type and $GR^{lck\text{-}Cre}$ mice, which lack GR expression in thymocytes (Mittelstadt et al., 2012). Surprisingly, two commonly used anti-GR monoclonal antibodies, 5E4 and BuGR2, had bright staining in GR-deficient thymocytes (70%–85% of wild-type; Figure S2B, left and center), making their use problematic. Another monoclonal antibody, G-5, had much lower background staining in GR-deficient thymocytes (30% of wild-type; Figure S2B, right) and was used in further studies. Corticosterone treatment of GR-deficient or wild-type thymocytes had no effect on GR levels as determined by staining

after fix-only (Figure 4A, left). However, as with GFP-GR 3617 cells, there was increased GR staining of wild-type perm-fixed thymocytes after corticosterone treatment (Figure 4A, right). Furthermore, detection of the GR increase in glucocorticoid-treated, perm-fixed thymocytes was found to be optimal under conditions similar to those used with GFP-GR-expressing cells (Figure S2C). GR staining intensity had a dose-dependent relationship with the concentration of glucocorticoids in perm-fixed mouse thymocytes (Figure 4B) and primary human T and B cells (Figure 4C). The results with mouse thymocytes were replicated with other monoclonal antibodies against the GR (Figure S2D). Imaging flow cytometry found that GR was nuclear in mouse thymocytes that were incubated in steroid-free medium and treated with fix-only (Figure 4D, top), consistent with previous exposure to glucocorticoids *in vivo*. In contrast, nuclear GR was lost after perm-fix (Figure 4D, bottom), indicating that the GR became unliganded after incubation in steroid-free medium. This interpretation was supported by detection of nuclear GR in thymocytes incubated with corticosterone prior to perm-fix (Figure 4D, bottom). GR staining intensity increased as a function of corticosterone concentration, and was bright in $CD4^{-}8^{-}$ double-negative (DN) thymocytes and dim in $CD4^{+}8^{+}$ double-positive (DP) thymocytes (Figure 4E), which reflects the previously documented difference in GR expression between these subsets (Brewer et al., 2002; Wiegers et al., 2001). To confirm that the kinetics of ligand-dependent GR detection after perm-fix were similar to those of chromatin interactions, chromatin immunoprecipitation (ChIP) of GR was performed on mouse thymocytes treated with corticosterone and subsequently washed twice and incubated at room temperature in steroid-free medium. GR association with the promoter of the glucocorticoid-responsive gene *Tsc22d3* (encoding the glucocorticoid-induced leucine zipper protein [Gilz]) was quantified in ChIP and chromatin input samples by qPCR (Figure S2E), and normalized to allow direct comparison with perm-fix results (Figure 4F). The glucocorticoid-induced signal rapidly decayed after glucocorticoid removal using either the perm-fix or ChIP assay, with calculated half-lives of 13 and 14 min, respectively. These were also similar to the half-life of GFP-GR in live or perm-fixed 3617 cells (Figure 2F). This result demonstrates that antibody staining of perm-fixed cells corresponds closely with temporal dynamics of GR-chromatin association measured by ChIP, rather than the dynamics of GR nuclear localization.

Permeabilization-Fixation Can Detect Differences in Tissue Glucocorticoid Concentrations

To examine glucocorticoid signaling in non-circulating cells, thymocytes and splenocytes from control mice or mice exposed to 45 min of handling stress were perm-fixed. Plasma corticosterone was higher in stressed compared with unstressed mice, and there was a corresponding increase in chromatin-associated GR staining across thymus and spleen lymphocyte subsets (Figure S3; Figure 5A). Wild-type mice were also compared with *Cyp11b1*-deficient mice, which have greatly diminished *de novo* glucocorticoid production (Mittelstadt et al., 2018). Corticosterone was reduced in $Cyp11b1^{-/-}$ compared with control mouse plasma, and there was a corresponding decrease in chromatin-associated GR staining across thymocyte subsets (Figure 5B, top). This decrease was not due to differential expression of GR protein, because total GR staining was similar in $Cyp11b1^{-/-}$ and control mice (Figure 5B, bottom). These results show that GR staining after perm-fix can identify endogenous differences in tissue corticosterone exposure.

A Ligand Titration Assay Quantitates Approximate Glucocorticoid Concentrations in Cultured Cells and Blood

Because there was a positive correlation between GR retention and glucocorticoid concentration, we reasoned that cells exposed to a given corticosterone concentration would have a certain perm-fix GR signal, and that this signal would increase only if they were subsequently exposed to a higher, but not lower, concentration of glucocorticoids *in vitro*. To test this, GFP-GR 3617 cells were cultured with known concentrations of corticosterone for 30 min (primary exposure), after which aliquots were distributed into 96-well plates and increasing concentrations of corticosterone were added (secondary exposure). After 5 min, the cells were perm-fixed and GFP-GR retention quantitated by flow cytometry (Figure 6A). The highest secondary steroid concentration at which the perm-fix GR signal did not increase should approximate the concentration in the primary exposure. We used a brief corticosterone treatment because the rapid loss of GR-chromatin interaction after ligand removal is expected to result in an underestimate of the actual primary glucocorticoid exposure. We found that an MFI (median fluorescence index) increase of ≥3% followed by a sustained increase in MFI could be used to identify the concentration of corticosterone in the primary culture. For example, when GFP-GR 3617 cells were cultured in the absence of glucocorticoids, the highest corticosterone concentration that did not result in an increased signal was 1 nM, indicating that 1 nM is the lower limit for the sensitivity of the secondary exposure titration assay (Figure 6B, left). Similarly, the signal in cells whose primary culture was in 3 nM corticosterone deviated from the baseline at a secondary concentration of ~8 nM (Figure 6B, center), and cells whose primary culture was in 100 nM corticosterone showed no consistent increase at any secondary corticosterone concentration, demonstrating that the plateau had been reached (≥100 nM) (Figure 6B, right). Flow cytometry-detected chromatin-associated GR may therefore be used to quantitatively estimate glucocorticoid exposure at the individual cell level within the physiologic range of 1–100 nM.

To determine whether perm-fix GR retention can be used to estimate exposure of primary cells to glucocorticoids *in vivo*, circulating blood was obtained from mice within 2 min of initial disturbance (baseline) or after 15 min of handling stress. Heparinized blood was aliquoted into different concentrations of corticosterone, incubated for 7.5–10 min at room temperature, and perm-fixed. As expected, exposure to a stressor increased total plasma corticosterone (from ~40 to ~540 nM; Figure 6C). Because the majority of plasma corticosterone is buffered by carrier proteins, we measured the free and therefore biologically active fraction, which after handling stress increased from ~3 to ~75 nM (Figure 6C). Using secondary ligand exposure and perm-fix, we found corresponding differences in GR staining patterns in circulating lymphocytes (Figure 6C, center). Under non-stress conditions, the estimated endogenous corticosterone exposure was calculated to be 9 nM, and after stress was ~75 nM (Figure 6C, right). These results show that perm-fix GR staining can quantitatively identify differences in corticosterone exposure *in vivo*, which correspond closely with the bioavailable glucocorticoid.

Identification and Approximate Quantitation of Cell-Targeted Delivery of Paracrine Glucocorticoids in the Thymus

Because thymocytes undergoing antigen-specific selection are affected by locally synthesized glucocorticoids (Mittelstadt et al., 2018), we asked whether differences in chromatin-associated GR could identify individual thymocytes being acted upon by paracrine-supplied glucocorticoids. We collected and immediately perm-fixed and then stained GR in thymocytes of post-natal day 1 control and *Cyp11b1*$^{foxn1\text{-}Cre}$ mice. TECs of *Cyp11b1*$^{foxn1\text{-}Cre}$ mice are unable to synthesize glucocorticoids, and antigen-induced apoptosis is increased in developing thymocytes (Mittelstadt et al., 2018). In the majority of thymocyte subsets, chromatin-associated GR levels were identical between control and *Cyp11b1*$^{foxn1\text{-}Cre}$ mice, indicating similar exposure to glucocorticoids *in vivo* (Figure 7A). However, in CD4^{+}8^{+}TCR^{hi} thymocytes, which have been activated by TCR signaling (Kearse et al., 1995), *Cyp11b1*$^{foxn1\text{-}Cre}$ mice had a clear reduction in chromatin-associated GR. These data suggest that TCR-signaled CD4^{+}8^{+} thymocytes, which represent the small fraction of total CD4^{+}8^{+} cells that recognize self-antigens (~5%), are acted on by TEC-synthesized glucocorticoids *in situ*. This cell specificity, moreover, demonstrates that TEC-derived glucocorticoids mediate their effect upon specific cells, rather than bathing the whole organ in uniformly elevated glucocorticoid levels. Because glucocorticoids antagonize thymocyte negative selection, the effect of TEC-derived glucocorticoids on key indicators of negative selection, PD-1 and Bim (Baldwin and Hogquist, 2007; Blank et al., 2003; Gray et al., 2012), was examined. The frequency of PD-1^{+}Bim^{+} cells was similar between the majority of wild-type and *Cyp11b1*$^{foxn1\text{-}Cre}$ thymocytes, but was elevated ~50% in CD4^{+}8^{+}TCR^{hi} thymocytes in *Cyp11b1*$^{foxn1\text{-}Cre}$ mice (Figure 7B), confirming that TEC-derived glucocorticoids act specifically on CD4^{+}8^{+}TCR^{hi} thymocytes, and that in their absence negative selection is enhanced in these cells. A ligand titration assay was performed to quantify exposure of thymocyte subpopulations to glucocorticoids. In these experiments we used thymocytes from mice in which the GR has been replaced by a GFP-GR fusion protein that is functionally indistinguishable from the endogenous GR (Brewer et al., 2002) (Figure S3), allowing us to directly measure GR levels. Thymocytes were aliquoted into wells whose medium contained the indicated corticosterone concentrations, incubated for 7.5 min at room temperature, and perm-fixed. CD4^{+}8^{+}TCR^{lo} (unselected) thymocytes were found to have been exposed to a glucocorticoid concentration of ~6 nM *in vivo* (Figure 7C). In contrast, the CD4^{+}8^{+}TCR^{hi} (responding to self; Kearse et al., 1995) were exposed to a 3-fold higher concentration (18 nM). Although not statistically significant, glucocorticoid levels perceived by CD4^{lo}8^{lo} thymocytes, which are enriched for cells that have been triggered via the TCR and are progressing to apoptosis, were slightly elevated compared with CD4^{+}8^{+}TCR^{lo} cells. CD4^{+}8^{-} and CD4^{-}8^{+} single positive, as well as mature splenic T and B cells, had glucocorticoid exposures similar to CD4^{+}8^{+}TCR^{lo} cells. These data confirm specific targeting of paracrine glucocorticoids to CD4^{+}8^{+}TCR^{hi} thymocytes and, more broadly, quantitative cell-specific heterogeneity in paracrine glucocorticoid signaling within an organ.

DISCUSSION

Activation of steroid receptors by their cognate ligands is important in myriad cellular processes, but detection, quantification, and even identification of these ligands and their cellular targets are major obstacles to investigating steroid function. Current methods are unable to quantitate ligand concentrations *in situ* with single-cell resolution, especially in situations where production may occur in a paracrine or autocrine manner. Ligand access to and activation of steroid receptors is even less clear. The technique outlined in this report has several distinct advantages over existing approaches. First, rather than detecting combined intra-cellular and extracellular ligands that may or may not be available to the receptor, it uses the receptor itself as a biosensor. Thus, factors that influence the effective ligand concentration, such as carrier proteins that act as buffers, the capacity to diffuse through membranes, and intracellular steroid metabolism, are accounted for, as shown by a tight correlation between the secondary exposure titration assay and free glucocorticoid levels in the plasma. Second, perm-fix primarily detects the liganded, chromatin-associated receptor fraction. Whereas nuclear shuttling of liganded cytosol-resident receptors (Giuliano et al., 1997) and expression of receptor target genes (Mittelstadt et al., 2018) have been used as indicators of steroid signaling, receptor export from the nucleus and mRNA degradation after ligand removal both take many hours (Liu and DeFranco, 2000; Yang et al., 2003). In contrast, perm-fix detection of the liganded receptor fraction, which was lost within minutes of ligand removal, results in high temporal resolution of receptor activity detection. GR retention in 3617 cells after perm-fix (9%–18% without and 39%–48% with glucocorticoid; see Figures 1 and 3) also roughly approximated the proportion of chromatin-bound GR as measured by single-molecule tracking in live 3617 cells (~13% without and ~44% with glucocorticoid) (Paakinaho et al., 2017). Third, the perm-fix method allows discrimination of effective ligand concentrations at the single-cell level. Fourth, because the perm-fix approach measures the consequences of receptor occupancy and not the ligand itself, it is ligand agnostic. Thus, where multiple hormone variants are available (as in the thymus; Taves et al., 2015, 2016a), perm-fix effectively measures the active concentration of the aggregate, which is ultimately what is biologically relevant. This implies that permfix could be used to detect the activity of nuclear receptors for which an endogenous ligand has not yet been identified. Finally, the perm-fix assay is simple, inexpensive, and rapid. It may be combined with other methods, such as fluorescence-activated cell sorting and ChIP, to study endogenous receptor promoter occupancy in different cell subsets from the same tissue sample.

The thymus is an organ in which paracrine production of glucocorticoids plays an important role in the generation of T cells essential for adaptive immunity. TCR occupancy on immature thymocytes leads to a continuum of responses depending upon affinity for the ligand, from death by neglect (low affinity) to survival (positive selection, moderate affinity) to activation-induced death (negative selection, high affinity). Glucocorticoids produced by a small number of TECs regulate this process by dampening TCR signals and promoting positive selection. This is demonstrated by two different genetic models, thymocyte GR deficiency or TEC Cyp11b1 deficiency. In both, reduced glucocorticoid signaling increases TCR-dependent apoptosis (negative selection) leading to an altered and ineffective TCR

repertoire (Mittelstadt et al., 2012, 2018). Although the requirement of glucocorticoids is clear, it has been thus far impossible to determine which cells are signaled by glucocorticoids, and thus how negative selection is antagonized. By using GR-chromatin binding as a biosensor, we have been able to show that glucocorticoid signaling occurs at a specific stage in thymocyte differentiation: $CD4^+8^+$ cells that have been stimulated by self-antigen as assessed by TCR upregulation. These observations address at least two long-standing questions about local glucocorticoid production. First, paracrine hormone delivery was highly targeted. The vast majority of thymocytes were exposed to the same low level of free corticosterone (~6 nM), with only $CD4^+8^+TCR^{hi}$ cells exposed to a higher concentration (~18 nM). This is consistent with the finding that in the absence of TEC glucocorticoid production, GR retention after perm-fix analysis was reduced specifically in this subset. Importantly, in this context in which glucocorticoids are supplied only by the circulation, these self-antigen-stimulated polyclonal thymocytes exhibited higher levels of markers indicating impending cell death, consistent with previous observations made in mice in which all thymocytes expressed the same positively selected transgenic TCR (Mittelstadt et al., 2018). Therefore, rather than being distributed throughout the organ, locally synthesized glucocorticoids were delivered directly to their biologically relevant targets. Because antigen presentation by TECs is the driver of positive selection, this direct delivery likely occurs because of physical proximity between the glucocorticoid-producing cell and the recipient cell. Delivery of lipophilic steroids across closely apposed membranes might be especially efficient, bypassing CBG and albumin in the interstitial fluid. Second, we conclude that a 3-fold elevation in ambient glucocorticoid levels is sufficient to skew antigen-induced negative selection toward positive selection for thymocytes bearing TCR with the appropriate affinity for self-antigen. This is particularly interesting because we previously found that a 50% decrease in thymocyte GR expression was sufficient to skew positive toward negative selection (Mittelstadt et al., 2012). It seems likely therefore that the biologically effective window for glucocorticoid-regulated thymocyte selection spans a 2- to 3-fold range of responsiveness.

We believe that the perm-fix technique developed here can be broadly applicable for the interrogation of paracrine and autocrine hormone signaling and more generally, transcription factor-chromatin interactions. In particular, the retention of histone H3 protein after perm-fix indicates that chromatin-cross-linking should be broadly useful for investigation of transcription factor activity. However, because the removal of ligand can result in rapid reversal of chromatin binding, detection of paracrine or autocrine signaling *in vivo* requires rapid cell collection. Thus, it is well suited for work with hematopoietic cells that can be easily dispersed from tissues. In situations where disruption of cell-cell interactions is more difficult, for example, in neural tissue, it might be useful to adapt this method by tissue perfusion with a perm-fix agent. This would have the added benefit of leaving organs intact, allowing visualization of cells in their normal anatomical context by microscopy. Alternatively, perm-fix treatment could be performed on cultured tissue sections, or other assays that specifically measure receptor-chromatin association (such as proximity ligation assay) might be used without the need for permeabilization. Such an approach might be used with fixed tissue biopsies from patients.

We have used the perm-fix approach to show cell-targeted delivery of paracrine glucocorticoids and to quantify intra-organ heterogeneity in active glucocorticoid concentrations. We hypothesize that this approach might be used to reveal similar “cytokine-like” behavior of steroids and other lipid molecules in multiple other organs and contexts. Basal and inducible expression of steroid metabolic enzymes suggests that targeted glucocorticoid signaling may occur in other lymphoid organs (Taves et al., 2015, 2016b) and barrier sites (Cima et al., 2004; Noti et al., 2010; Slominski et al., 2005), and the identification of glucocorticoid target cells in these tissues is important to understand homeostatic regulation of immunity and inflammation. Furthermore, as targeted glucocorticoid therapies begin to enter clinical use (Buttgereit et al., 2005), identification of optimal glucocorticoid target cells may greatly improve the efficacy and risk profiles of glucocorticoid treatments.

STAR★METHODS

CONTACT FOR REAGENT AND RESOURCE SHARING

Further information and requests for resources and reagents should be directed to and will be fulfilled by the Lead Contact, Jonathan D. Ashwell (jda@pop.nci.nih.gov).

EXPERIMENTAL MODEL AND SUBJECT DETAILS

Cell Culture—3617 cells were cultured in DMEM (GIBCO) supplemented with 10% heat-inactivated FBS, 2 mM L-glutamine, 50 μM 2-mercaptoethanol, 100 μg/ml gentamicin, and 5 μg/ml tetracycline. The 3617 cell line is derived from the 3134 mouse mammary adenocarcinoma line. 3617 cells stably expressed a GFP-tagged wild-type mouse GR (GFP-GR) or a dimerization-impaired GR mutant containing the A465T/I634A amino acid substitutions (GFP-GR^{mon}) under the control of a tetracycline-repressible promoter, or were GR-deficient (KO). Additional 3617 lines stably expressed a GPF-tagged androgen receptor (GFP-AR), an mCherry-tagged estrogen receptor α (mCh-ER), or GFP-tagged progesterone receptor β (GFP-PR) under the control of a tetracycline-repressible promoter. All 3617 lines and mutant receptors have been previously described (Presman et al., 2016). Prior to experiments, 3617 cells were cultured overnight in DMEM supplemented with 10% charcoal-stripped heat-inactivated FBS, L-glutamine, 2-mercaptoethanol, and gentamicin (as above) but no tetracycline. Primary mouse cells and PBMCs were cultured in RPMI 1640 (GIBCO) supplemented with 10% FBS, 2 mM L-glutamine, 50 μM 2-mercaptoethanol, and 100 μg/ml gentamicin. Prior to experiments, cells were cultured for at least one hour in RPMI 1640 containing 10% charcoal-stripped heat-inactivated FBS, L-glutamine, 2-mercaptoethanol, and gentamicin (as above).

Mice—Wild-type C57BL/6 mice were obtained from Jackson Laboratories. Mice with *Lck* promoter-driven T cell GR deletion (*GR*$^{lck\text{-}Cre}$) (Mittelstadt et al., 2012), *Actb* promoter-driven global *Cyp11b1* deletion (*Cyp11b1*$^{-/-}$) (Mittelstadt et al., 2018), or *Foxn1* promoter-driven TEC *Cyp11b1* deletion (*Cyp11b1*$^{foxn1\text{-}Cre}$) (Mittelstadt et al., 2018) were generated by us and have been described previously. GFP-GR knockin mice were the kind gift of Dr. Louis J. Muglia (Brewer et al., 2002). Mice were between five and eight weeks of age unless otherwise specified. We were unable to detect any sex differences and therefore pooled

female and male mice for all analyses. Mice were kept on a 12:12 light:dark cycle, with *ad lib* access to standard chow (NIH-31, Teklad). To stimulate an endogenous corticosterone response, mice were held by the scruff of the neck for approximately 15 s, transfered to a new, lidless cage and left on the benchtop for 10 min, and again helf by the scruff of the neck for 15 s. These “stress” exposed mice were euthanized 15 min after initial disturbance of the home cage. For experiments examining endogenous glucocorticoids (basal or stress-induced) mice were collected between 10 am and 3 pm (Zeitgeiber time 4 to 9). All protocols and procedures were approved by the NCI Animal Care and Use Committee and followed the NIH Guide for the Care and Use of Laboratory Animals guidelines.

METHOD DETAILS

Flow Cytometry—For experiments using 3617 or HEK293 cells, approximately 10^6 cells were aliquoted into a V-bottom 96-well plate, centrifuged, the supernatant decanted, and the cells resuspended in 100 μL of ice-cold fixative. For determination of chromatin-associated protein by permeabilization-fixation, samples were fixed with FoxP3 transcription factor fixation buffer (eBioscience) or FACS buffer (PBS containing 2% charcoal-stripped FBS, 0.5% bovine serum albumin, and 0.05% sodium azide) with 2% formaldehyde (Sigma, 252549) and 0.5% Triton X-100 (Fluka) for 20 min at room temperature. For determination of total intracellular protein by fixation alone, samples were fixed with Cytofix/Cytoperm (BD Biosciences) or FACS buffer containing 2% formaldehyde for 20 min at room temperature. Samples were then diluted and washed with ice-cold permeabilization buffer (eBioscience) or FACS buffer containing 0.1% Triton X-100, and in some cases incubated with intracellular staining antibodies (1:100) on ice for 30 min and then washed twice with the same buffer. Cells were then resuspended in FACS buffer and data were obtained using LSR Fortessa SORP and FACS Canto II flow cytometers with FACSDiva software (BD Biosciences) and analyzed with FlowJo software (TreeStar). Median fluorescence intensity (MFI) was used for all analyses. We occasionally compared median and mean fluorescence intensities, and results were nearly identical. For experiments using fresh primary cells, tissues were dispersed in PBS containing 2% charcoal-stripped FBS, and approximately 5×10^6 cells were aliquoted into tubes and resuspended in 125 μL of ice-cold perm-fix or total fix, incubated for 20 min at room temperature, and washed with permeabilization buffer as above. Unless otherwise specified, intracellular GR staining was done overnight at 4° (antibodies diluted 1:100) with an Alexa 488 or Alexa-647 conjugated mouse monoclonal antibodie (G-5, Santa Cruz). Cells were then washed twice and resuspended in FACS buffer. Surface markers were stained for at least 30 min on ice (antibodies diluted 1:200 – 1:300), cells washed, and data obtained and analyzed as described above. For ligand titration analysis to estimate endogenous glucocorticoid exposure, cells were quickly dissociated and diluted in 50 μl of PBS containing 2% FBS with various corticosterone concentrations. After a brief incubation at room temperature, cells were diluted with 250 ul of ice-cold perm-fix buffer, incubated 20 min at room temperature, and washed and stained as described above. For imaging flow cytometry, 2 μM DAPI was added to fixed and fix-perm treated cells, data were obtained using an ImageStream Mark II flow cytometer (Amnis), and analysis performed using IDEAS software (Amnis). Analyses were performed on all collected data, and representative images were selected from cells gated to include approximately 5% of cells spanning the GR MFI value or median nuclear translocation score for a given cell

population. Relative nuclear translocation was quantified using the Similarity Score in IDEAS, using the formula $S = \ln[(1+\rho)/(1-\rho)]$, where S is the similarity score and ρ is the Pearson correlation coefficient comparing GFP pixel intensities between GFP and DAPI images of the same cell. For measurement of lymphocyte GR-chromatin association *in situ*, thymi were dispersed in FACS buffer and immediately perm-fixed for 25 min at room temperature. Cells were then washed with permeabilization buffer, stained for intracellular and surface proteins, and data acquired on a flow cytometer. Gating strategies used to analyze blood, spleen, and thymus cells are demonstrated in (Figure S3).

Western Blot—Cell samples were boiled in SDS sample buffer for 10 min, proteins separated by SDS-PAGE, transferred (Trans-Blot Turbo, Bio-Rad), blots blocked with 5% dried milk (Bio-Rad), incubated overnight with primary antibodies against GR (G-5), β-actin (AC-15), or Histone H3 (D2B12) and detected with HRP-conjugated secondary antibodies and enhanced chemiluminescence substrate (SuperSignal West Dura, Thermo) using a ChemiDoc imaging system (Bio-Rad).

ChIP—ChIP was performed using SimpleChIP kit reagents (Cell Signaling, 9003) according to the manufacturer's protocol. 15×10^6 mouse thymocytes were treated with 10^{-6} M corticosterone, cross-linked for 10 min with 1% methanol-free formaldehyde at room temperature on a rocker, and quenched with glycine for 5 min. Cells were washed twice with ice-cold PBS containing complete pro-tease inhibitor cocktail (Roche, Complete), resuspended in cell lysis buffer (kit Buffer A), and incubated 10 min on ice with regular mixing. Nuclei were pelleted and washed in nuclei lysis buffer (kit Buffer B), chromatin resuspended in nuclei lysis buffer and digested with 1000 gel units of micrococcal nuclease at 37° with periodic mixing by inversion. Digestion was stopped by adding EDTA to 50 mM and chilling in ice. Pelleted nuclei were resuspended in ChIP buffer (kit reagent), incubated 10 min on ice, sonicated in a QSonica Q800R2 (10 s on, 25% amplitude), and chromatin aliquoted to different tubes (input controls and ChIP samples). Samples (5×10^6 cells per reaction) were brought to 500 μL with ChIP buffer, rotated overnight at 4° with a rabbit anti-mouse GR monoclonal antibody (D8H2, Cell Signaling), rotated for 2 h with 30 μL of Protein G magnetic beads (kit reagent), washed three times with ChIP buffer, and washed once with high salt buffer. Samples were then incubated in 150 μL ChIP elution buffer (kit) for 30 min at 65° at 1200 rpm, supernatant cross-links reversed for 2 h at 65° with 200 mM NaCl and 2 μL Proteinase K (20 mg/ml), and DNA purified with QIAquick PCR purification columns (QIAGEN). Quantitative PCR for the *Tsc22d3* gene (encoding the glucocorticoid-induced GILZ protein) promoter was performed on a QuantStudio 6 system (Applied Biosystems) using PowerUp SYBR Green Master Mix (Applied Biosystems) with forward primer 5′-TGGTGCCAAATGTCAAGAAG-3′ and reverse primer 5′-TATGTTTGCCTGAGCCCTCT-3′.

Reagents—Corticosterone (Sigma), cortisol (Sigma), 17β-estradiol (Sigma), progesterone (Sigma), and testosterone (Nutritional Biochemicals) were kept as 10^{-2} M stocks in ethanol at −20°C and diluted immediately before being used in experiments.

QUANTIFICATION AND STATISTICAL ANALYSIS

Glucocorticoid Quantification—Plasma corticosterone was measured using a commercial chemiluminescent immunoassay kit (Arbor Assays, K014). For total corticosterone, 5 μL of plasma was incubated with 5 μL of dissociation reagent, diluted with 490 μL assay buffer, and assayed in duplicate according to the manufacturer's instructions. For free corticosterone, plasma samples were loaded into Microcon Ultracel YM-10 filters (Millipore, 42406), centrifuged 10,000 × g for 30 min at room temperature, and corticosterone was measured in the filtrate (free corticosterone), retentate (bound corticosterone), and in unfiltered plasma (total corticosterone). Quantification of cellular corticosterone exposure was performed using a secondary exposure ligand titration assay. Cell aliquots were treated with increasing amounts of corticosterone and GR retention was quantified by flow cytometry. An MFI increase of ≥ 3% from the previous concentration followed by further sustained increases in MFI was used to identify the first concentration greater than the primary exposure, and the concentration preceding this ≥ 3% increase was considered to be the corticosterone concentration in the primary exposure.

Statistical Analysis—Analyses were performed using GraphPad Prism software. K_D and B_{max} values were calculated using the saturation one-site total binding function, and using the saturation – one-site specific binding on specific binding data gave nearly identical results. GR-chromatin half-life values were calculated using the dissociation – one phase exponential decay function. Thymocyte and splenocyte glucocorticoid concentrations were compared using a Kruskal-Wallis test followed by Dunn's test for multiple comparisons. Error bars indicate SEM unless otherwise stated and significance was set at $p < 0.05$. All experiments were performed at least twice, and replicates and sample numbers are indicated in the figure captions.

Supplementary Material

Refer to Web version on PubMed Central for supplementary material.

ACKNOWLEDGMENTS

This work was supported by the Intramural Research Program of the Center for Cancer Research, National Cancer Institute, NIH, and by a CIHR Postdoctoral Fellowship (MFE179782) to M.D.T. The authors wish to thank Drs. Ferenc Livak, Caiyi C. Li, and David Stephany for help with imaging flow cytometry and cell sorting; Bhuvana Pandalai for technical assistance; Dr. Louis J. Muglia for the gift of the GFP-GR knockin mice; and Dr. Diana A. Stavreva for critical review of the manuscript.

REFERENCES

Amateau SK, Alt JJ, Stamps CL, and McCarthy MM (2004). Brain estradiol content in newborn rats: sex differences, regional heterogeneity, and possible de novo synthesis by the female telencephalon. Endocrinology 145, 2906–2917. [PubMed: 14988386]

Attardi B, and Ohno S (1976). Androgen and estrogen receptors in the developing mouse brain. Endocrinology 99, 1279–1290. [PubMed: 991821]

Baldwin TA, and Hogquist KA (2007). Transcriptional analysis of clonal deletion in vivo. J. Immunol 179, 837–844. [PubMed: 17617574]

Blank C, Brown I, Marks R, Nishimura H, Honjo T, and Gajewski TF (2003). Absence of programmed death receptor 1 alters thymic development and enhances generation of CD4/CD8 double-negative TCR-transgenic T cells. J. Immunol 171, 4574–4581. [PubMed: 14568931]

Brewer JA, Sleckman BP, Swat W, and Muglia LJ (2002). Green fluores-cent protein-glucocorticoid receptor knockin mice reveal dynamic receptor modulation during thymocyte development. J. Immunol 169, 1309–1318. [PubMed: 12133953]

Buttgereit F, Burmester GR, and Lipworth BJ (2005). Optimised glucocorticoid therapy: the sharpening of an old spear. Lancet 365, 801–803. [PubMed: 15733723]

Cima I, Corazza N, Dick B, Fuhrer A, Herren S, Jakob S, Ayuni E, Mueller C, and Brunner T (2004). Intestinal epithelial cells synthesize glucocorticoids and regulate T cell activation. J. Exp. Med 200, 1635–1646. [PubMed: 15596520]

Cobice DF, Mackay CL, Goodwin RJA, McBride A, Langridge-Smith PR, Webster SP, Walker BR, and Andrew R (2013). Mass spectrometry imaging for dissecting steroid intracrinology within target tissues. Anal. Chem 85, 11576–11584. [PubMed: 24134553]

Croft AP, O'Callaghan MJ, Shaw SG, Connolly G, Jacquot C, and Little HJ (2008). Effects of minor laboratory procedures, adrenalectomy, social defeat or acute alcohol on regional brain concentrations of corticosterone. Brain Res. 1238, 12–22. [PubMed: 18755165]

Forment JV, and Jackson SP (2015). A flow cytometry-based method to simplify the analysis and quantification of protein association to chromatin in mammalian cells. Nat. Protoc 10, 1297–1307. [PubMed: 26226461]

Giuliano KA, DeBiasio RL, Dunlay RT, Gough A, Volosky JM, Zock J, Pavlakis GN, and Taylor DL (1997). High-Content Screening: A New Approach to Easing Key Bottlenecks in the Drug Discovery Process. J. Biomol. Screen 2, 249–259.

Gray DH, Kupresanin F, Berzins SP, Herold MJ, O'Reilly LA, Bouillet P, and Strasser A (2012). The BH3-only proteins Bim and Puma cooperate to impose deletional tolerance of organ-specific antigens. Immunity 37, 451–462. [PubMed: 22960223]

Ha T, Kozlov AG, and Lohman TM (2012). Single-molecule views of protein movement on single-stranded DNA. Annu. Rev. Biophys 41, 295–319. [PubMed: 22404684]

Hoffman EA, Frey BL, Smith LM, and Auble DT (2015). Formaldehyde crosslinking: a tool for the study of chromatin complexes. J. Biol. Chem 290, 26404–26411. [PubMed: 26354429]

Htun H, Holth LT, Walker D, Davie JR, and Hager GL (1999). Direct visualization of the human estrogen receptor alpha reveals a role for ligand in the nuclear distribution of the receptor. Mol. Biol. Cell 10, 471–486. [PubMed: 9950689]

Kearse KP, Takahama Y, Punt JA, Sharrow SO, and Singer A (1995). Early molecular events induced by T cell receptor (TCR) signaling in immature CD4+ CD8+ thymocytes: increased synthesis of TCR-alpha protein is an early response to TCR signaling that compensates for TCR-alpha instability, improves TCR assembly, and parallels other indicators of positive selection. J. Exp. Med 181, 193–202. [PubMed: 7528767]

Lechner O, Wiegers GJ, Oliveira-Dos-Santos AJ, Dietrich H, Recheis H, Waterman M, Boyd R, and Wick G (2000). Glucocorticoid production in the murine thymus. Eur. J. Immunol 30, 337–346. [PubMed: 10671188]

Liu J, and DeFranco DB (2000). Protracted nuclear export of glucocorticoid receptor limits its turnover and does not require the exportin 1/CRM1-directed nuclear export pathway. Mol. Endocrinol 14, 40–51. [PubMed: 10628746]

Mittelstadt PR, Monteiro JP, and Ashwell JD (2012). Thymocyte responsiveness to endogenous glucocorticoids is required for immunological fitness. J. Clin. Invest 122, 2384–2394. [PubMed: 22653054]

Mittelstadt PR, Taves MD, and Ashwell JD (2018). Cutting Edge: De Novo Glucocorticoid Synthesis by Thymic Epithelial Cells Regulates Antigen-Specific Thymocyte Selection. J. Immunol 200, 1988–1994. [PubMed: 29440508]

Mochizuki N, Yamashita S, Kurokawa K, Ohba Y, Nagai T, Miyawaki A, and Matsuda M (2001). Spatio-temporal images of growth-factor-induced activation of Ras and Rap1. Nature 411, 1065–1068. [PubMed: 11429608]

Munck A, and Brinck-Johnsen T (1968). Specific and nonspecific physico-chemical interactions of glucocorticoids and related steroids with rat thymus cells in vitro. J. Biol. Chem 243, 5556–5565. [PubMed: 5699052]

Noti M, Sidler D, and Brunner T (2009). Extra-adrenal glucocorticoid synthesis in the intestinal epithelium: more than a drop in the ocean? Semin. Immunopathol 31, 237–248. [PubMed: 19495759]

Noti M, Corazza N, Mueller C, Berger B, and Brunner T (2010). TNF suppresses acute intestinal inflammation by inducing local glucocorticoid synthesis. J. Exp. Med 207, 1057–1066. [PubMed: 20439544]

Overk CR, Perez SE, Ma C, Taves MD, Soma KK, and Mufson EJ (2013). Sex steroid levels and AD-like pathology in 3xTgAD mice. J. Neuroendocrinol 25, 131–144. [PubMed: 22889357]

Paakinaho V, Presman DM, Ball DA, Johnson TA, Schiltz RL, Levitt P, Mazza D, Morisaki T, Karpova TS, and Hager GL (2017). Single-molecule analysis of steroid receptor and cofactor action in living cells. Nat. Commun 8, 15896. [PubMed: 28635963]

Philibert D, and Raynaud JP (1973). Progesterone binding in the immature mouse and rat uterus. Steroids 22, 89–98. [PubMed: 4353432]

Presman DM, Ogara MF, Stortz M, Alvarez LD, Pooley JR, Schiltz RL, Grøntved L, Johnson TA, Mittelstadt PR, Ashwell JD, et al. (2014). Live cell imaging unveils multiple domain requirements for in vivo dimerization of the glucocorticoid receptor. PLoS Biol. 12, e1001813. [PubMed: 24642507]

Presman DM, Ganguly S, Schiltz RL, Johnson TA, Karpova TS, and Hager GL (2016). DNA binding triggers tetramerization of the glucocorticoid receptor in live cells. Proc. Natl. Acad. Sci. USA 113, 8236–8241. [PubMed: 27382178]

Prior NH, Heimovics SA, and Soma KK (2013). Effects of water restriction on reproductive physiology and affiliative behavior in an opportunistically-breeding and monogamous songbird, the zebra finch. Horm. Behav 63, 462–474. [PubMed: 23274698]

Reul JM, and de Kloet ER (1985). Two receptor systems for corticosterone in rat brain: microdistribution and differential occupation. Endocrinology 117, 2505–2511. [PubMed: 2998738]

Russo-Marie F, Paing M, and Duval D (1979). Involvement of glucocorticoid receptors in steroid-induced inhibition of prostaglandin secretion. J. Biol. Chem 254, 8498–8504. [PubMed: 468838]

Schmidt KL, and Soma KK (2008). Cortisol and corticosterone in the song-bird immune and nervous systems: local vs. systemic levels during development. Am. J. Physiol. Regul. Integr. Comp. Physiol 295, R103–R110. [PubMed: 18353885]

Slominski A, Zbytek B, Szczesniewski A, Semak I, Kaminski J, Sweat-man T, and Wortsman J (2005). CRH stimulation of corticosteroids production in melanocytes is mediated by ACTH. Am. J. Physiol. Endocrinol. Metab 288, E701–E706. [PubMed: 15572653]

Stavreva DA, Wiench M, John S, Conway-Campbell BL, McKenna MA, Pooley JR, Johnson TA, Voss TC, Lightman SL, and Hager GL (2009). Ultradian hormone stimulation induces glucocorticoid receptor-mediated pulses of gene transcription. Nat. Cell Biol 11, 1093–1102. [PubMed: 19684579]

Taves MD, Gomez-Sanchez CE, and Soma KK (2011a). Extra-adrenal glucocorticoids and mineralocorticoids: evidence for local synthesis, regulation, and function. Am. J. Physiol. Endocrinol. Metab 301, E11–E24. [PubMed: 21540450]

Taves MD, Ma C, Heimovics SA, Saldanha CJ, and Soma KK (2011b). Measurement of steroid concentrations in brain tissue: methodological considerations. Front. Endocrinol. (Lausanne) 2, 39. [PubMed: 22654806]

Taves MD, Plumb AW, Sandkam BA, Ma C, Van Der Gugten JG, Holmes DT, Close DA, Abraham N, and Soma KK (2015). Steroid profiling reveals widespread local regulation of glucocorticoid levels during mouse development. Endocrinology 156, 511–522. [PubMed: 25406014]

Taves MD, Losie JA, Rahim T, Schmidt KL, Sandkam BA, Ma C, Silversides FG, and Soma KK (2016a). Locally elevated cortisol in lymphoid organs of the developing zebra finch but not Japanese quail or chicken. Dev. Comp. Immunol 54, 116–125. [PubMed: 26366679]

Taves MD, Plumb AW, Korol AM, Van Der Gugten JG, Holmes DT, Abraham N, and Soma KK (2016b). Lymphoid organs of neonatal and adult mice preferentially produce active glucocorticoids from metabolites, not precursors. Brain Behav. Immun 57, 271–281. [PubMed: 27165988]

Thévenot DR, Toth K, Durst RA, and Wilson GS (2001). Electrochemical biosensors: recommended definitions and classification. Biosens. Bio-electron 16, 121–131.

Tobiansky DJ, Korol AM, Ma C, Hamden JE, Jalabert C, Tomm RJ, and Soma KK (2018). Testosterone and corticosterone in the mesocorticolimbic system of male rats: effects of gonadectomy and caloric restriction. Endocrinology 159, 450–464. [PubMed: 29069423]

Vacchio MS, Papadopoulos V, and Ashwell JD (1994). Steroid production in the thymus: implications for thymocyte selection. J. Exp. Med 179, 1835–1846. [PubMed: 8195711]

Van Engelenburg SB, and Palmer AE (2008). Fluorescent biosensors of protein function. Curr. Opin. Chem. Biol 12, 60–65. [PubMed: 18282482]

Wang Y, Botvinick EL, Zhao Y, Berns MW, Usami S, Tsien RY, and Chien S (2005). Visualizing the mechanical activation of Src. Nature 434, 1040–1045. [PubMed: 15846350]

Wasner G, Hennermann I, and Kratochwil K (1983). Ontogeny of mesenchymal androgen receptors in the embryonic mouse mammary gland. Endocrinology 113, 1771–1780. [PubMed: 6605242]

Weikum ER, Knuesel MT, Ortlund EA, and Yamamoto KR (2017). Glucocorticoid receptor control of transcription: precision and plasticity via allostery. Nat. Rev. Mol. Cell Biol 18, 159–174. [PubMed: 28053348]

Wiegers GJ, Knoflach M, Böck G, Niederegger H, Dietrich H, Falus A, Boyd R, and Wick G (2001). CD4(+)CD8(+)TCR(low) thymocytes express low levels of glucocorticoid receptors while being sensitive to glucocorticoid-induced apoptosis. Eur. J. Immunol 31, 2293–2301. [PubMed: 11477541]

Yang E, van Nimwegen E, Zavolan M, Rajewsky N, Schroeder M, Magnasco M, and Darnell JE, Jr. (2003). Decay rates of human mRNAs: correlation with functional characteristics and sequence attributes. Genome Res. 13, 1863–1872. [PubMed: 12902380]

Yeakley JM, Balasubramanian K, and Harrison RW (1980). Comparison of glucocorticoid-receptor binding kinetics with predictions from a biomolecular model. J. Biol. Chem 255, 4182–4188. [PubMed: 7372674]

Zhang J, Wang X, Cui W, Wang W, Zhang H, Liu L, Zhang Z, Li Z, Ying G, Zhang N, and Li B (2013). Visualization of caspase-3-like activity in cells using a genetically encoded fluorescent biosensor activated by protein cleavage. Nat. Commun 4, 2157. [PubMed: 23857461]

Highlights

- Paracrine glucocorticoid signaling is critical in thymocyte development
- Permeabilization-fixation retains active steroid receptors, quantifying ligand levels
- Thymus-derived glucocorticoids specifically target antigen-signaled thymocytes

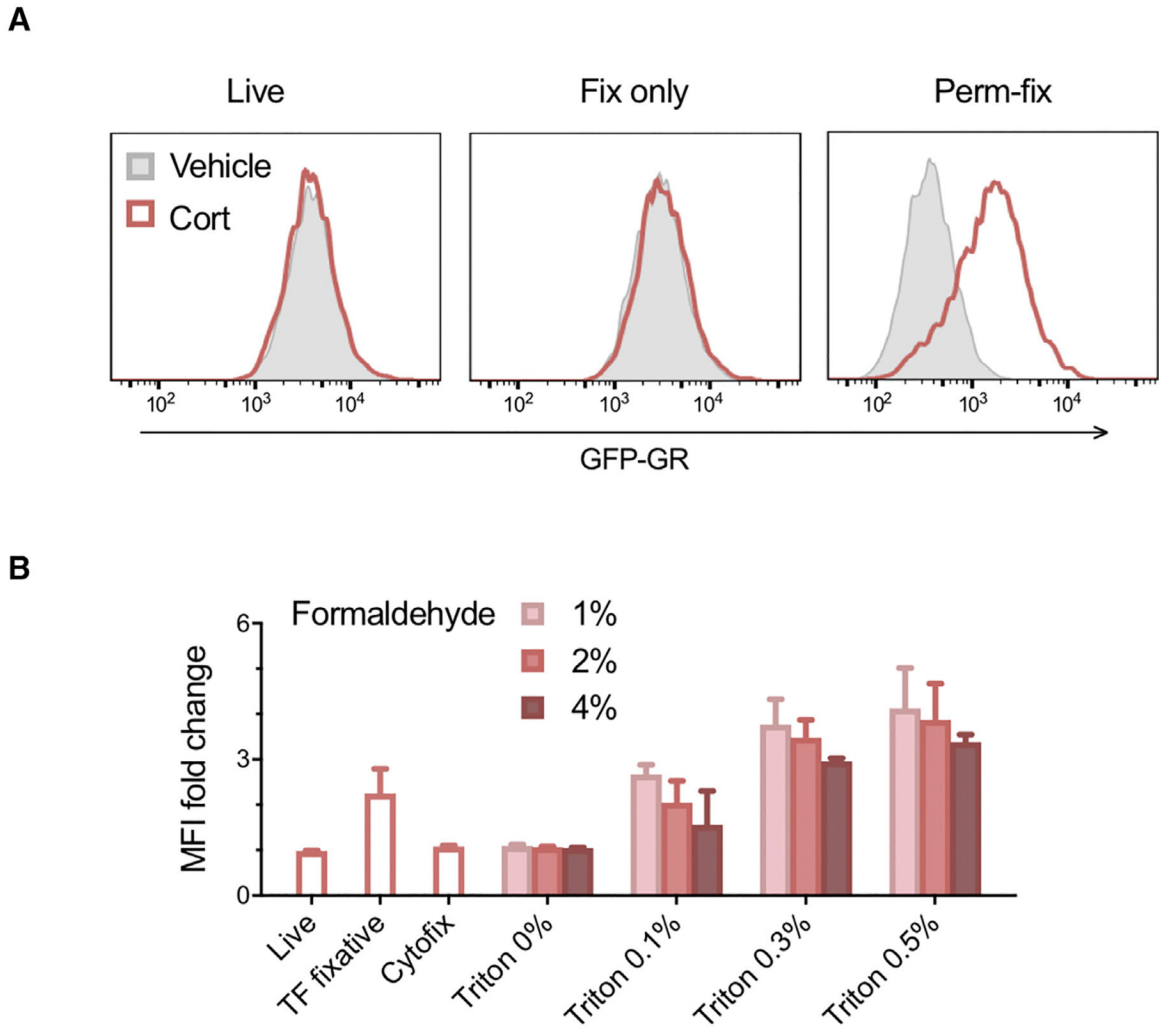

Figure 1. Simultaneous Permeabilization and Fixation Preferentially Retains the Liganded Glucocorticoid Receptor

(A) 3617 mouse mammary adenocarcinoma cells expressing a GFP-tagged glucocorticoid receptor (GR) were incubated in the absence or presence of the GR ligand corticosterone for 15 min. Cells were then kept on ice (Live), fixed with 2% paraformaldehyde in fluorescence-activated cell sorting (FACS) buffer (Fix only), or fixed with 0.5% Triton X-100 and 2% paraformaldehyde in FACS buffer (Perm-fix). Cells were washed and GFP-GR quantified by flow cytometry. Histograms are representative of two independent experiments.

(B) Relative increase in GR content of GFP-GR 3617 cells upon addition of corticosterone, after perm-fix with various buffers. Data are geometric means of two independent experiments ± geometric SD.

Cort, corticosterone; MFI, median fluorescence index; Triton, Triton X-100.

See also Figure S1.

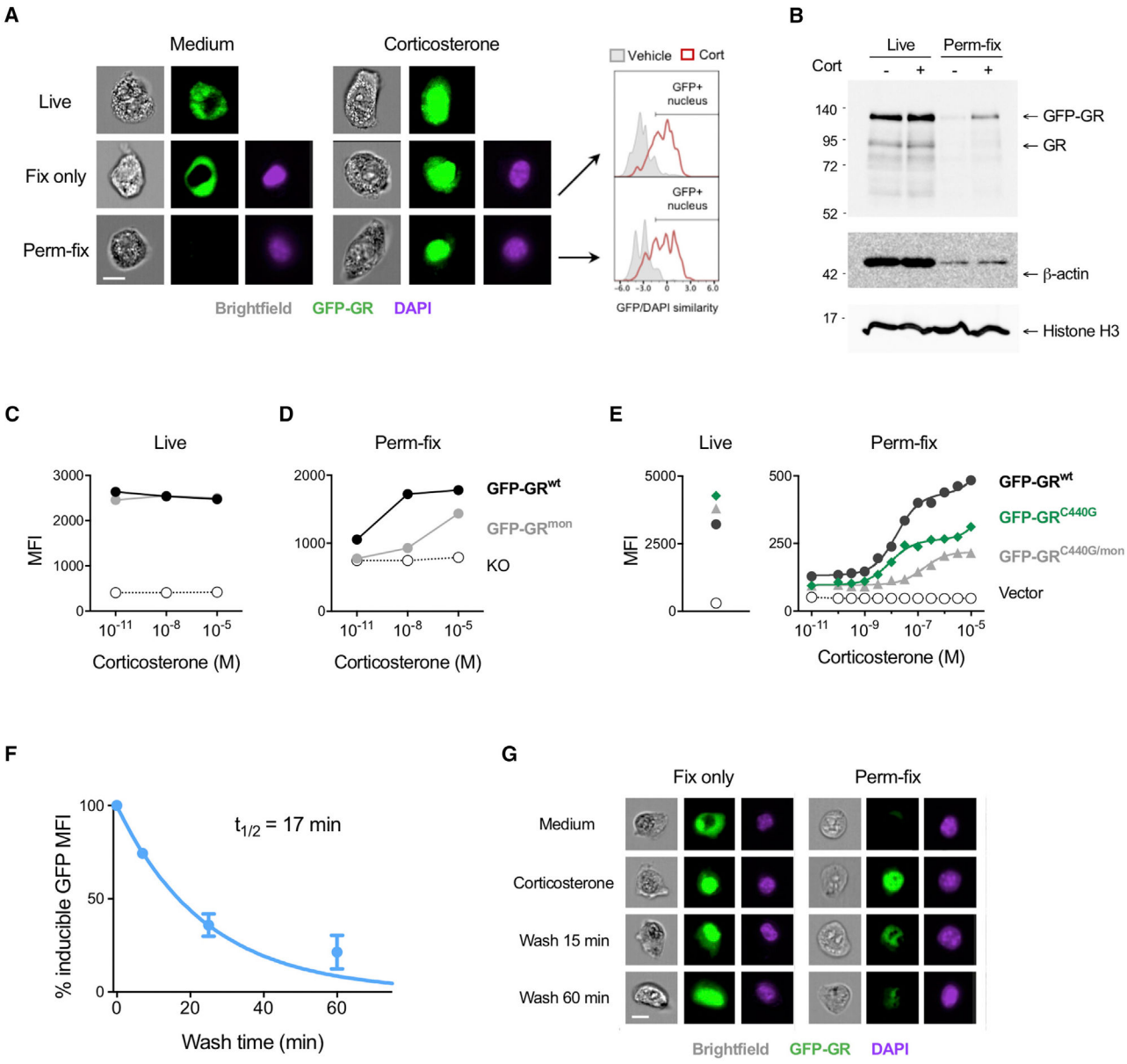

Figure 2. Permeabilization-Fixation Retains Chromatin-Associated GRs

(A) GFP-GR 3617 cells were treated with corticosterone, kept on ice (Live), fixed or perm-fixed, and data were acquired by imaging flow cytometry. DAPI staining was used to define the nucleus after fix or perm-fix. Frequencies of GR^{+} nuclei were quantified using the similarity score algorithm included in the IDEAS analysis software. Images are from cells with the median GFP/DAPI similarity score from each sample. Data are representative of three independent experiments. Scale bar, 10 μm.

(B) GFP-GR 3617 cells were treated with corticosterone, perm-fixed, washed, diluted in SDS gel loading buffer, subjected to SDS-PAGE, and immunoblotted for the indicated proteins. Blots are representative of two independent experiments.

(C and D) 3617 cells expressing the wild-type GR ($GFP\text{-}GR^{wt}$), dimerization-impaired GR ($GFP\text{-}GR^{mon}$), or deficient for GR (KO) were treated with different concentrations of

corticosterone, kept on ice (C), or perm-fixed (D), and data were acquired by flow cytometry. Data are representative of two independent experiments.

(E) HEK293T cells were transfected with plasmids encoding the wild-type GR (GFP-GR^{wt}), GR C440G mutant (GR^{C440G}), which has reduced DNA binding, or the $GR^{C440G/mon}$ double mutant. GFP^{+} cells were sorted, treated with different concentrations of corticosterone, and perm-fixed, and data were acquired by flow cytometry. Live cells were untreated. Data are representative of three independent experiments.

(F) GFP-GR 3617 cells were treated with corticosterone for 15 min and then incubated in steroid-free medium for the indicated times and perm-fixed, and data were acquired by flow cytometry. The GR MFI of cells perm-fixed in the presence of corticosterone was set to 100%, and the MFI of cells kept in steroid-free medium was set to 0%. Data are means ± SEM of three independent experiments.

(G) GFP-GR 3617 cells were treated with corticosterone, incubated in steroid-free medium for 15 min, and perm-fixed, and data were acquired by imaging flow cytometry. Data are representative of two independent experiments. Scale bar, 10 μm.

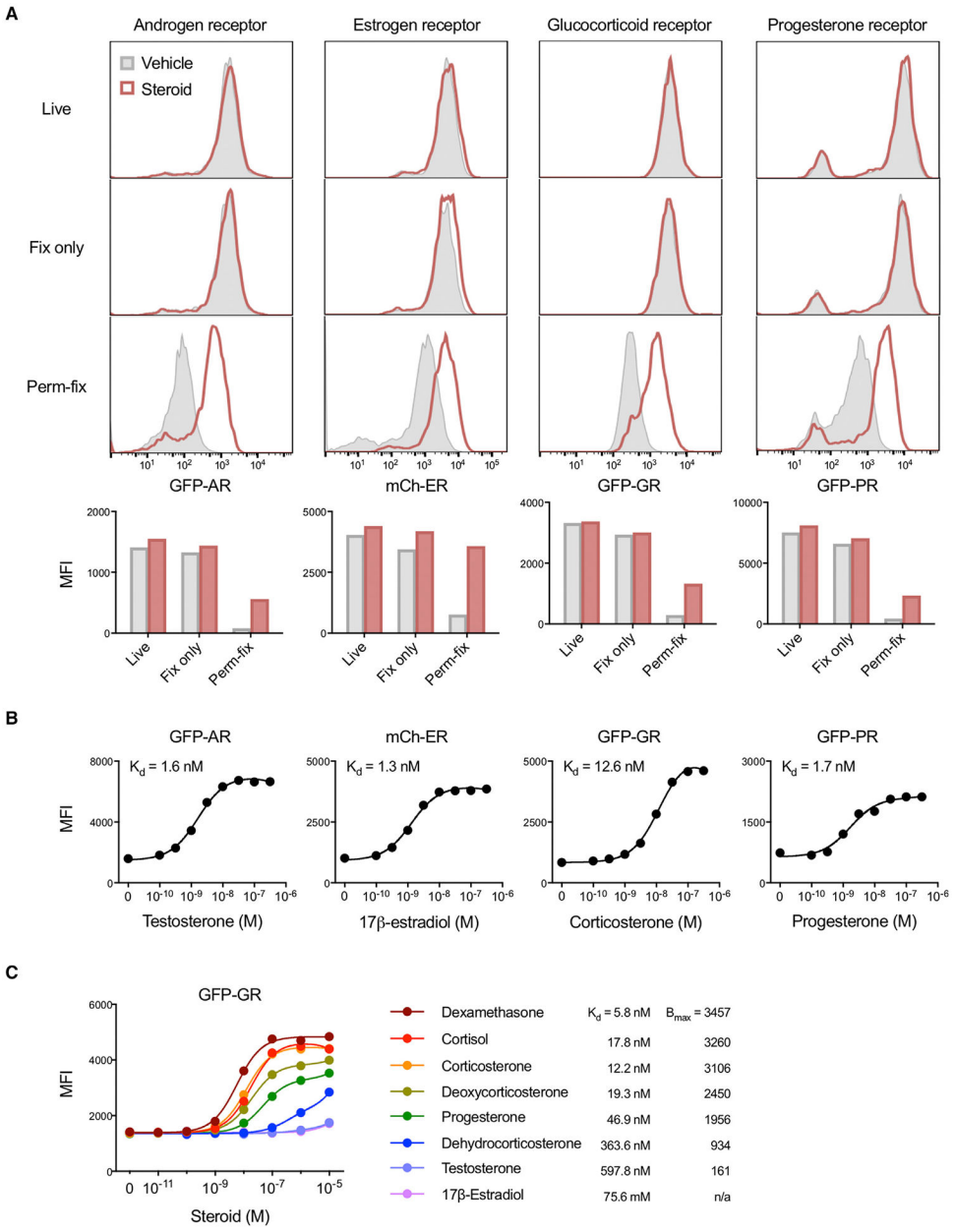

Figure 3. Crosslinking of Liganded Nuclear Receptors Quantifies Ligand Exposure

(A) 3617 cells expressing a GFP-androgen receptor, mCherry-estrogen receptor α, GFP-GR, or GFP-progesterone receptor β were incubated with their cognate steroid ligands (testosterone, 17β-estradiol, corticosterone, or progesterone) and then kept on ice (Live), fixed, or perm-fixed. Cells were quantified by flow cytometry. Horizontal axis scales are identical in stacked histograms of the same column. Data are representative of four independent experiments.

(B) 3617 cells expressing nuclear receptor fusion proteins were treated with various steroid concentrations, perm-fixed, and measured by flow cytometry. Data are representative of two independent experiments.

(C) GFP-GR 3617 cells were treated with different steroids, perm-fixed, and measured by flow cytometry. Data are representative of two independent experiments.
AR, androgen receptor; B_{max}, maximum binding; ER, estrogen receptor α; GR, glucocorticoid receptor; PR, progesterone receptor β; MFI, median fluorescence index.

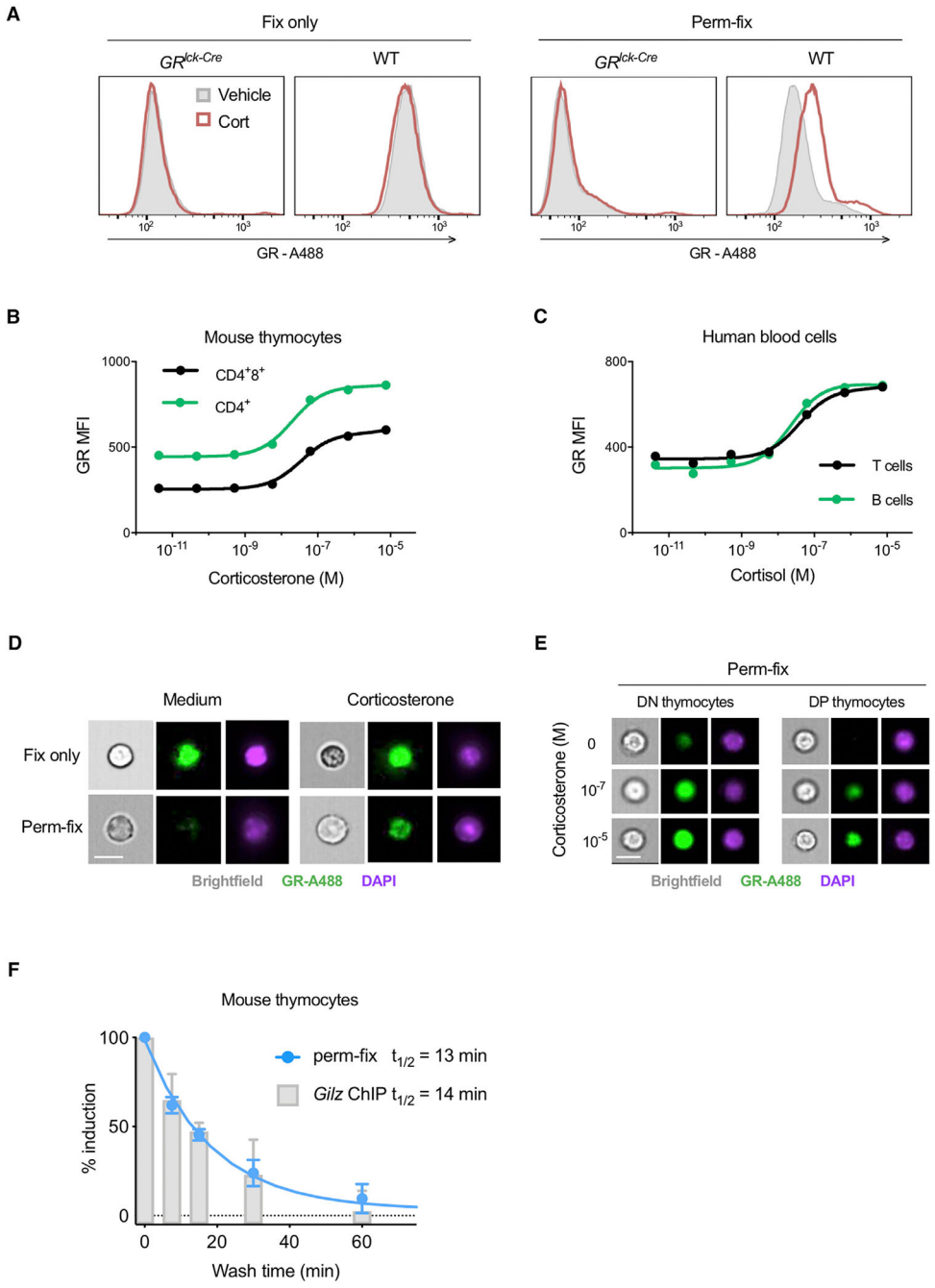

Figure 4. Permeabilization-Fixation of Primary Cells Allows Antibody Detection of Chromatin-Associated GR

(A) Primary thymocytes from mice with T lymphocyte-specific deletion of the GR (*GR*$^{lck\text{-}Cre}$) or wild-type (WT) mice were treated with corticosterone, fixed or perm-fixed, and stained for GR, and data were acquired by flow cytometry. Data are representative of two independent experiments.

(B and C) Primary mouse thymocytes (B) or primary human peripheral blood mononuclear cells (C) were treated with various glucocorticoid concentrations, surface stained, perm-fixed, and measured by flow cytometry. Estimated K_d values are 39 and 26 nM for mouse

$CD4^+8^+$ and $CD4^+$ thymocytes and 39 and 22 nM for human T and B cells, respectively. Data are representative of two independent experiments.

(D) WT mouse thymocytes were treated with corticosterone, surface stained, and fixed or perm-fixed, and data were acquired by imaging flow cytometry. Data are representative of two independent experiments. Scale bars, 10 μm.

(E) WT mouse thymocytes were treated with different corticosterone concentrations, surface stained, perm-fixed, and data were acquired by imaging flow cytometry. Data are representative of two independent experiments. Scale bars, 10 μm.

(F) WT mouse thymocytes were incubated for 20 min in medium containing 10^{-7} M corticosterone, then washed twice and incubated in steroid-free medium for the indicated times. One aliquot of cells was then fixed in 1% formaldehyde and ChIP-qPCR performed (as described in STAR Methods) to quantitate GR binding to the *Tsc22d3* (Gilz) gene promoter, and another aliquot was perm-fixed, GR stained, and counted by flow cytometry. Data from both assays were normalized by setting the corticosterone-treated (unwashed) sample equal to 100% induction and the corticosterone-untreated sample set equal to 0% induction. Data are means ±SEM of three mice in two independent experiments.

See also Figure S2.

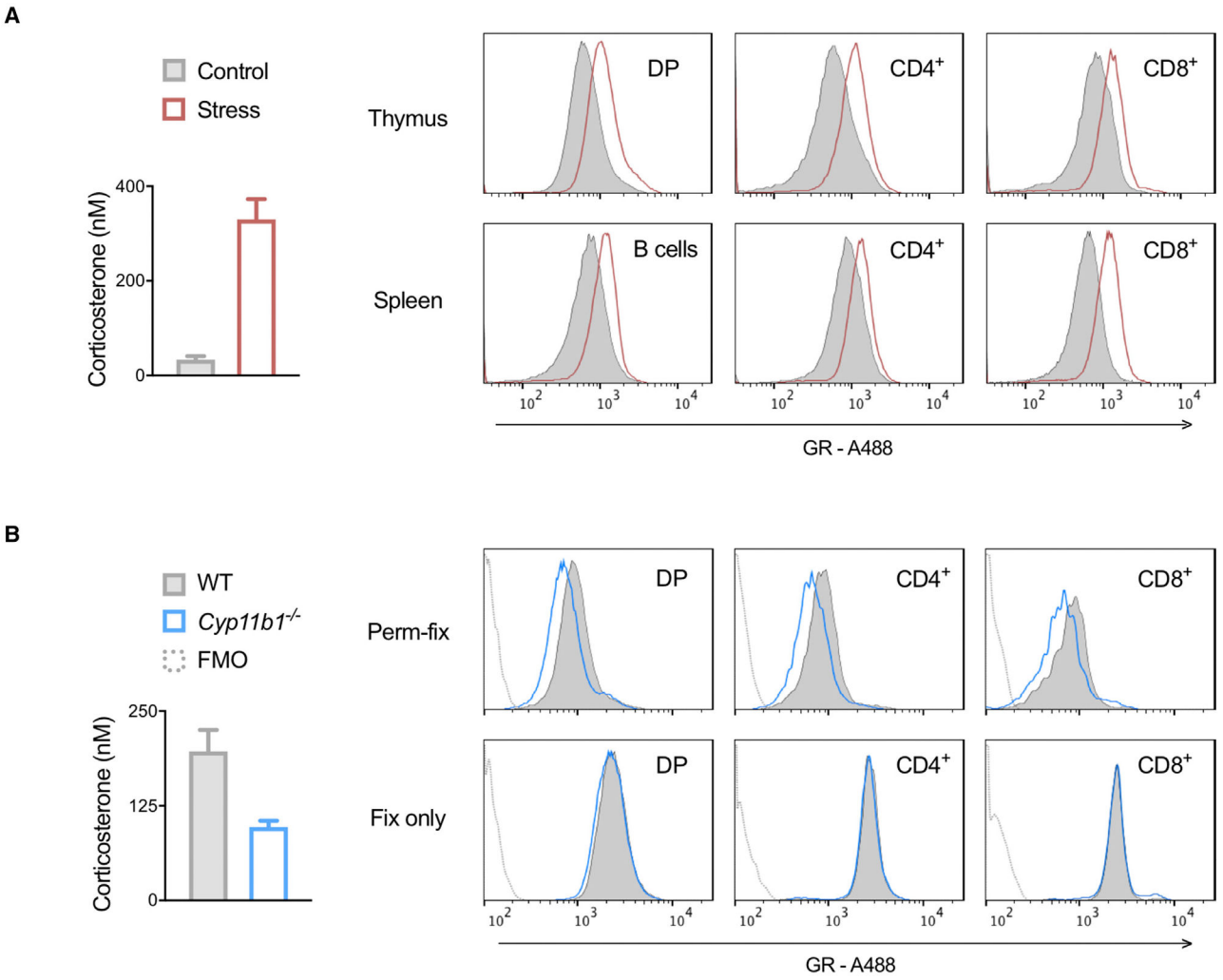

Figure 5. Chromatin-Associated GR Can Be Used to Detect Tissue and Cell-Specific Glucocorticoid Differences *In Vivo*

(A and B) Plasma and tissue samples were collected from (A) undisturbed or stressed (handling and movement) WT mice or (B) WT and Cyp11b1-deficient mice. Total plasma corticosterone levels were quantified by immunoassay and means ± SD of duplicate measurements are shown in bar graphs. Cells were perm-fixed, GR stained, and surface markers stained, and data were acquired by flow cytometry, shown in histograms. Data are representative of three independent experiments. FMO, fluorescence minus one (no anti-GR antibody) control.

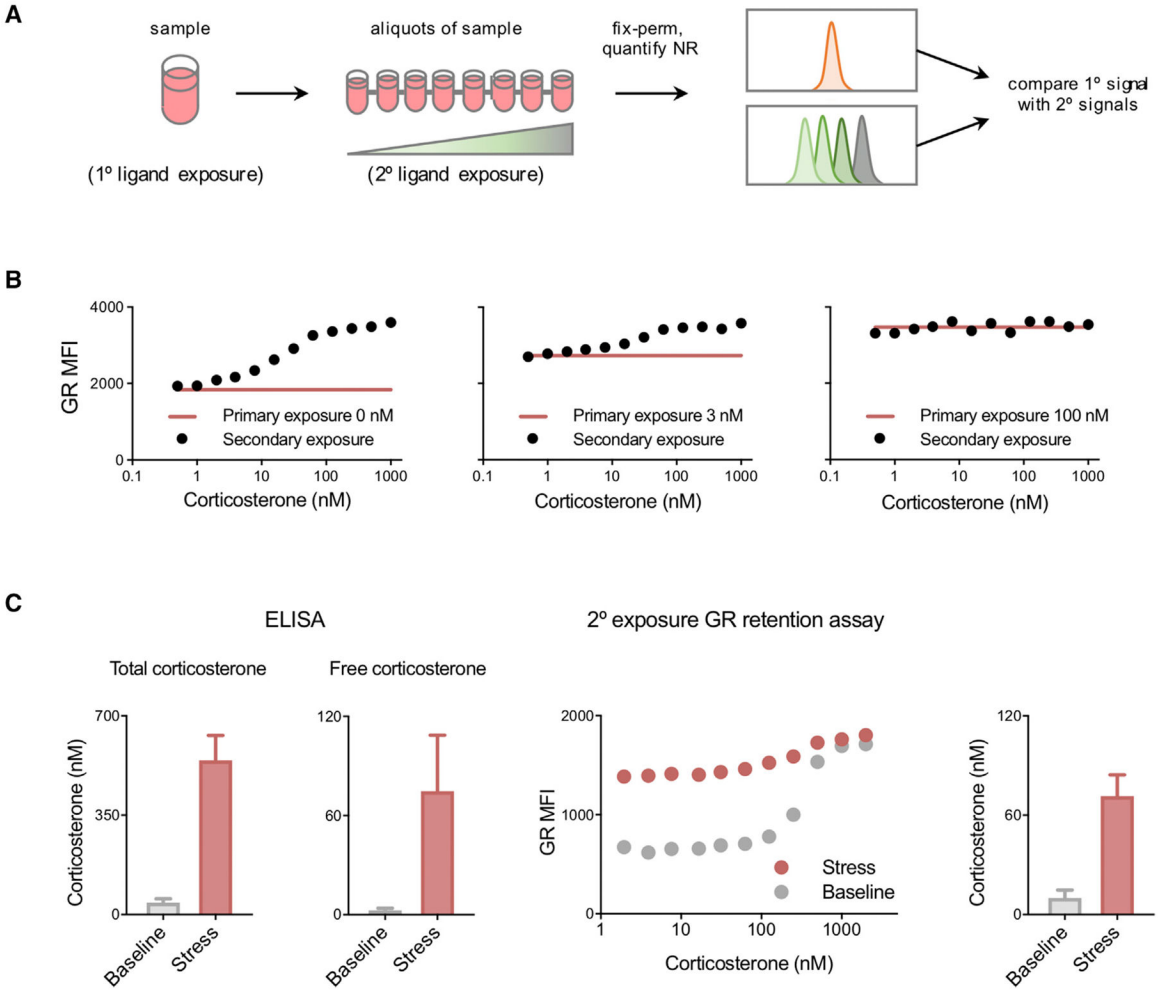

Figure 6. Glucocorticoid Measurement by Ligand Titration Assay

(A) Protocol for estimation of corticosterone exposure. Cells were cultured in 0, 3, or 100 nM corticosterone (primary exposure), then divided into aliquots and treated with various corticosterone concentrations (secondary exposure). Cells were then perm-fixed, and data were acquired by flow cytometry.

(B) GFP-GR 3617 cells treated as described above. Data are representative of two independent experiments.

(C) Blood samples were collected from mice immediately after disturbance (<2 min, n = 6) or after 15 min of handling stress (n = 5) and divided into aliquots. Plasma was isolated, and total and free corticosterone were quantified by immunoassay (left two panels). Blood was incubated with the indicated corticosterone concentrations, perm-fixed, and stained, and data were acquired by flow cytometry (secondary exposures, right panels). The corticosterone concentrations shown in the rightmost panel were calculated using B cells as described in the STAR Methods. Data are presented as means ± SEM.

See also Figure S3.

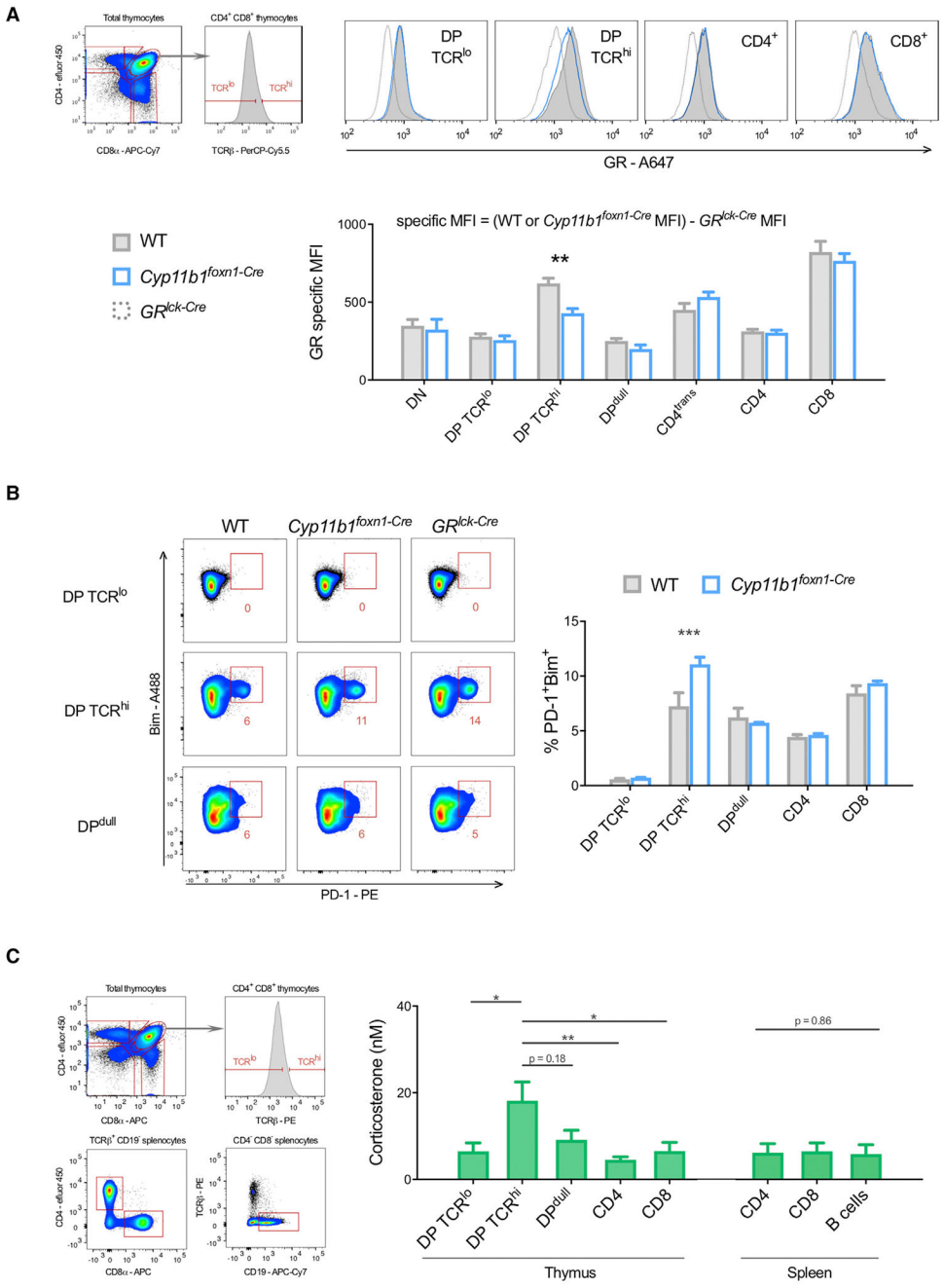

Figure 7. Targeted Delivery of TEC-Derived Glucocorticoids in the Thymus

(A) Thymi were collected from neonatal WT (n = 6) and *Cyp11b1*$^{\text{foxn1-Cre}}$ (n = 3) littermates; cells were perm-fixed, GR stained, and surface markers stained, and data were acquired by flow cytometry. Specific MFI is the result of subtracting the non-specific staining of the same thymocyte subpopulation from *GR*$^{lck\text{-}Cre}$ mice, which lack GR expression (WT or *Cyp11b1*$^{\text{foxn1-Cre}}$ MFI – *GR*$^{lck\text{-}Cre}$ MFI). Data are representative of three independent experiments. CD4$^{\text{trans}}$, transitional (CD4^{+}CD8$^{\text{lo}}$); DN, CD4^{-}8^{-}; DP, CD4^{+}8^{+}; DP$^{\text{dull}}$, CD4$^{\text{lo}}$8$^{\text{lo}}$; ISP, immature single positive (CD8^{+}TCR^{-}).

(B) Thymi were collected from WT (n = 3) and *Cyp11b1*$^{foxn1\text{-}Cre}$ (n = 3) immediately after disturbance, cells dispersed, surface markers stained, fixed, permeabilized, intracellular proteins stained, washed, and data acquired by flow cytometry. Subsets were compared using a two-way ANOVA and Sidak's test for multiple comparisons. DP, $CD4^{+}8^{+}$; DP^{dull}, $CD4^{lo}8^{lo}$.

(C) Thymus and spleen were collected from mice (n = 6) immediately after disturbance, cells dispersed, and aliquots immediately incubated with a range of corticosterone concentrations for 7.5 min, perm-fixed, stained, and data acquired by flow cytometry. The corticosterone concentrations shown in the bar graph were calculated as described in STAR Methods, and subsets were compared using a Kruskal-Wallis test and Dunn's test for multiple comparisons.

DP, $CD4^{+}8^{+}$; DP^{dull}, $CD4^{lo}8^{lo}$.

All bar graphs show means ± SEM with significance indicated by *$p < 0.05$, **$p < 0.01$, and ***$p < 0.001$.

See also Figure S3.

KEY RESOURCES TABLE

REAGENT or RESOURCE	SOURCE	IDENTIFIER
Antibodies		
Anti-mouse B220 (clone RA3–6B2)	BD PharMingen	Cat# 553090
Anti-mouse Bim (clone C34C5)	Cell Signaling Technology	Cat# 2933; RRID: AB_1030947
Anti-mouse CD4 (clone RM4–5)	eBioscience	Cat# 47-0042-82; RRID: AB_1272183
Anti-mouse CD4 (clone GK1.5)	eBioscience	Cat# 48-0041-82; RRID: AB_1272194
Anti-mouse CD8 (clone 53–6.7)	BD PharMingen	Cat# 553035; RRID: AB_398527
Anti-mouse CD19 (clone 1D3)	BD PharMingen	Cat# 553786; RRID: AB_395050
Anti-mouse CD69 (clone H1.2F3)	eBioscience	Cat# 25-0691-82; RRID: AB_469637
Anti-mouse Histone H3 (clone D2B12)	Cell Signaling Technology	Cat# 4620; RRID: AB_1904005
Anti-mouse PD-1 (clone J43)	eBioscience	Cat# 12-9985-82; RRID: AB_466295
Anti-mouse TCRb (clone H57–597)	BD PharMingen	Cat# 560657; RRID: AB_1727575
Anti-mouse Ter119 (clone Ter-119)	Biolegend	Cat# 116207; RRID: AB_313708
Anti-human CD3 (clone HIT3a)	eBioscience	Cat# 12-0039-42; RRID: AB_10853029
Anti-human CD19 (clone HIB19)	eBioscience	Cat# 56-0199-42; RRID: AB_2043819
Anti-β-actin (clone AC-15)	Sigma	Cat# A5441; RRID: AB_476744
Anti-GR (clone G-5)	Santa Cruz	Cat# sc-393232; RRID: AB_2687823
Anti-GR (clone D8H2)	Cell Signaling Technology	Cat# 12007; RRID: AB_11179215
Anti-GR (clone BuGR2)	Novus	Cat# NB300–731; RRID: AB_608643
Anti-GR (clone 5E4)	US Biological	Cat# G3030-01M
Chemicals, Peptides, and Recombinant Proteins		
16% Formaldehyde solution	Thermo	Cat# 28908
Corticosterone	Sigma	Cat# 27840
Cortisol	Sigma	Cat# H-4001
Cytofix/Cytoperm fixation/permeabilization kit	BD Biosciences	Cat# 554722
Dehydrocorticosterone	Steraloids	Cat# Q3690-000
Deoxycorticosterone	Sigma	Cat# D6875
Dexamethasone	Sigma	Cat# D1756
Formaldehyde solution	Sigma	Cat# 252549–25ML
PowerUp SYBR Green Master Mix	Applied Biosystems	Cat# A25742
Progesterone	Sigma	Cat# P-0130
Testosterone	Nutritional Biochemicals	Cat# 103010
Transcription factor staining buffer set	eBioscience	Cat# 00-5523-00
Triton X-100 solution	Fluka	Cat# 93443
Critical Commercial Assays		
Corticosterone Chemiluminescent Immunoassay	Arbor Assays	Cat# K014
SimpleChIP Enzymatic Chromatin IP Kit	Cell Signaling Technology	Cat# 9003S
SuperSignal West Dura Substrate	Thermo	Cat# 34075
Experimental Models: Cell Lines		
Mouse: 3617 GFP-AR cells	Presman et al., 2016	N/A
Mouse: 3617 GFP-GR^{wt} cells	Presman et al., 2016	N/A

REAGENT or RESOURCE	SOURCE	IDENTIFIER
Mouse: 3617 GFP-GR^{mon} cells	Presman et al., 2016	N/A
Mouse: 3617 GR$^{-/-}$ cells	Presman et al., 2016	N/A
Mouse: 3617 GFP-PR cells	Presman et al., 2016	N/A
Mouse: 3617 mCherry-ER cells	Presman et al., 2016	N/A
Human: HEK293T cells	ATCC	CRL-3216; RRID: CVCL_0063
Experimental Models: Organisms/Strains		
C57BL/6J mice	The Jackson Laboratory	Jax: 000664; RRID: IMSR_JAX:000664
Cyp11b1$^{actin\text{-}Cre}$ mice	Mittelstadt et al., 2018	N/A
Cyp11b1$^{foxn1\text{-}Cre}$ mice	Mittelstadt et al., 2018	N/A
GFP-GR mice	Brewer et al., 2002	N/A
GR$^{lck\text{-}Cre}$ mice	Mittelstadt et al., 2012	Jax: 021021; RRID: IMSR_JAX:021021
Oligonucleotides		
Primer: *Tsc22d3* forward: TGGTGCCAAATGTCAAGAAG	This paper	N/A
Primer: *Tsc22d3* reverse: TATGTTTGCCTGAGCCCTCT	This paper	N/A
Recombinant DNA		
Plasmid: GFP-GR^{wt}	Paakinaho et al., 2017	N/A
Plasmid: GFP-GR^{mon}	Paakinaho et al., 2017	N/A
Plasmid: GFP-GR^{C440G}	Paakinaho et al., 2017	N/A
Plasmid: GFP-GR$^{mon/C440G}$	Paakinaho et al., 2017	N/A
Software and Algorithms		
FlowJo	TreeStar	https://www.flowjo.com/
IDEAS	Amnis	https://www.luminexcorp.com/imaging-flow-cytometry/
Image Lab	Bio-Rad	http://www.bio-rad.com/
Prism	GraphPad Software	https://www.graphpad.com/